vol. 174, no. 1 the american naturalist july 2009

E-Article

Transition from Connected to Fragmented Vegetation across an Environmental Gradient: Scaling Laws in Ecotone Geometry

Michael T. Gastner,[1,*] Beata Oborny,[2] D. K. Zimmermann,[2] and Gunnar Pruessner[3]

1. Institute for Chemistry and Biology of the Marine Environment, Carl von Ossietzky Universität Oldenburg, Carl-von-Ossietzky-Straße 9–11, 26111 Oldenburg, Germany; and Santa Fe Institute, 1399 Hyde Park Road, Santa Fe, New Mexico 87501; 2. Department of Plant Taxonomy and Ecology, Loránd Eötvös University, Pázmány Péter sétány 1/C, H-1117, Budapest, Hungary; 3. Mathematics Institute, University of Warwick, Gibbet Hill Road, Coventry CV4 7AL, United Kingdom; and Department of Mathematics, Imperial College London, 180 Queen's Gate, London SW7 2BZ, United Kingdom

Submitted May 9, 2008; Accepted December 29, 2008; Electronically published May 8, 2009

abstract: A change in the environmental conditions across space—for example, altitude or latitude—can cause significant changes in the density of a vegetation type and, consequently, in spatial connectivity. We use spatially explicit simulations to study the transition from connected to fragmented vegetation. A static (gradient percolation) model is compared to dynamic (gradient contact process) models. Connectivity is characterized from the perspective of various species that use this vegetation type for habitat and differ in dispersal or migration range, that is, "step length" across the landscape. The boundary of connected vegetation delineated by a particular step length is termed the " hull edge." We found that for every step length and for every gradient, the hull edge is a fractal with dimension 7/4. The result is the same for different spatial models, suggesting that there are universal laws in ecotone geometry. To demonstrate that the model is applicable to real data, a hull edge of fractal dimension 7/4 is shown on a satellite image of a piñon-juniper woodland on a hillside. We propose to use the hull edge to define the boundary of a vegetation type unambiguously. This offers a new tool for detecting a shift of the boundary due to a climate change.

Keywords: patch dynamics, landscape connectivity, environmental gradient, tree line, fractal geometry.

Introduction

The distribution of vegetation across environmental gradients has received considerable attention since the beginnings of vegetation science, for example, in gradient analysis (Whittaker and Niering 1965). Interest in this topic increased further after reports of significant shifts in vegetation boundaries (e.g., tree lines) due to recent climate changes (Allen and Breshears 1998; Danby and Hik 2007). Detecting boundary shifts has been suggested for biomonitoring climate change (Kimball and Weihrauch 2000; but see Zeng and Malanson 2006 and references therein).

Because the geometries of most natural vegetation boundaries are complicated, it is not self-evident what to measure, that is, which feature of a boundary could be sufficiently general to enable comparisons between years and/or geographic regions. Observing the vegetation along a gradient, for example, from lower to higher altitudes across an alpine tree line, often reveals a complex pattern of patches. Inside the forest zone, a relatively high cover of forest is interspersed with gaps of various sizes. The average gap size typically increases toward the edge, where small gaps become large enough to coalesce. At that point, the forest becomes fragmented. Farther uphill, the sizes of fragments decrease and the forest vegetation vanishes; see the map in Zeng and Malanson (2006). Apart from alpine tree lines, the same general pattern has also been documented at the edges of a gallery forest (map in Loehle et al. 1996) and of piñon-juniper woodlands (map in Milne et al. 1996). Several studies have emphasized that natural boundaries are not straight lines but gradual ("soft"; Forman 1995), with a transition zone (ecotone) of considerable spatial extent.

In this article, we study the geometry of this transition zone with spatially explicit numerical simulations. Our main objective is to model the effect of smooth changes in environmental conditions. Moving along a gradient, the density of a particular vegetation type (e.g., forest) decreases. A decrease in density inevitably leads to fragmentation. An abrupt change from the connected to the fragmented state occurs even along a smooth gradient. This phenomenon is studied here with gradient percolation models. The simplest case is the gradient random map (GRM). There, the probability that a site will be occupied by a certain vegetation type changes continuously through space, without correlations between the states of different sites. This model is static, in the sense that it does not

* Corresponding author; e-mail: mgastner@gmail.com.

Am. Nat. 2009. Vol. 174, pp. E23–E39.
DOI: 10.1086/599292

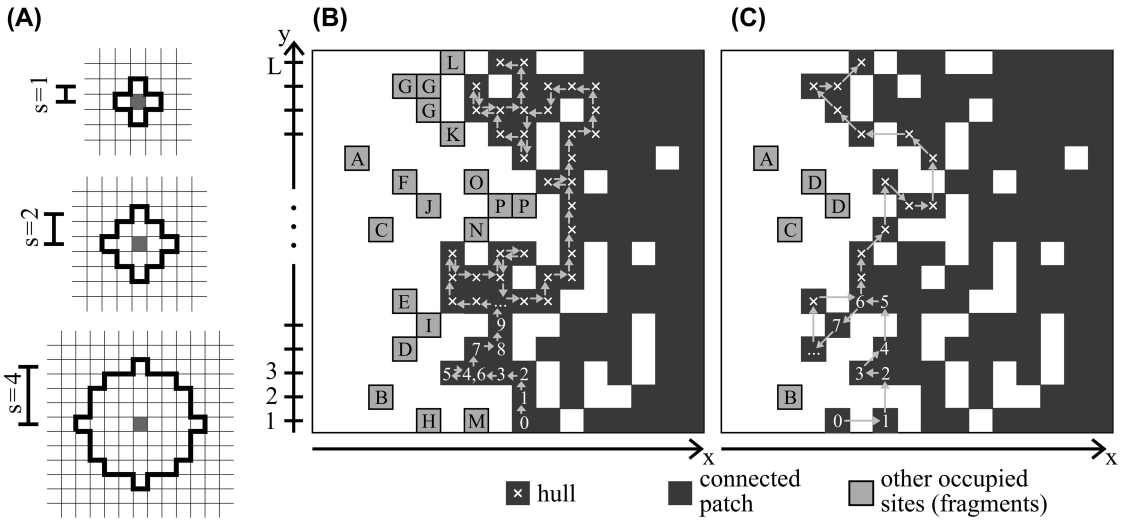

Figure 1: *A*, Examples of percolation neighborhoods. Suppose the gray site in the center is occupied. If any other site within the highlighted neighborhood is occupied, it belongs to the same patch as the gray site when the maximum step length s is 1 (*top*), 2 (*middle*), or 4 (*bottom*). *B*, Definition of the hull edge for $s = 1$. The hull edge can be delineated using a left-turning biased walk, which finds the leftmost path within the connected patch (for details, see "Determination of the Hull Edge by a Biased Walk"). Numbers and crosses mark the steps along the path. *C*, Hull edge for $s = 2$. Now the walk can skip over some vacant sites along the way. Relative to *B*, the boundary shifts to the left, and fewer fragments remain. Distinct fragments are labeled with different letters.

account for the dynamics of site occupancy. As a step toward more realism, we also investigate the gradient contact process (GCP), in which local colonization and extinction events are modeled explicitly and a dynamic boundary is investigated. We assume that the colonization distance is limited, so that the states of adjacent sites are correlated.

In both the GRM and the GCP, space is represented by a square lattice, and only two states of the lattice sites, vacant and occupied, are distinguished. We analyze the spatial pattern of occupied sites from the perspective of a species that moves (i.e., migrates or disperses) across this patchy landscape. We assume that two occupied sites are connected and hence belong to the same vegetation patch if and only if the species can move from one site to the other without stepping on a vacant site in between. Crossing a vacant area is possible, but residence (i.e., ending the step there) is not permitted. Various step lengths are tested, and the environmental gradient is also varied.

This organism-centered description of the landscape allows us to analyze connectivity on various spatial scales. Both empirical and modeling studies have emphasized that the same landscape can be connected or fragmented, depending on the movement range of the actual species (Forman 1995; Ims 1995; With and Crist 1995; With et al. 1997; Wiens 1997; Solé and Bascompte 2006). For example, an area with wetland patches in North Carolina was found to be connected for mink (*Mustela vison*; dispersal range ≈ 25 km) but fragmented for prothonotary warblers (*Prothonotaria citrea*; dispersal range mostly <12 km; Bunn et al. 2000). By changing the step length in the simulations, we can test whether species with different dispersal ranges experience different geometries.

For each step length, we determine which sites are connected and hence belong to the same patch (i.e., percolation cluster). The largest patch is generally the one that connects the highest number of sites in the region of low density to the region of highest density. If the gradient points along the horizontal x-direction from sparse to full vegetation cover, this patch will span from the bottom to the top of the lattice (fig. 1), a property that can be used in delineating the edge. The probability of two distinct large patches in the densest region is negligible in a sufficiently large lattice. Therefore, we call the largest patch the "connected patch." All the other patches we call "fragments." Finally, we delineate the connected patch's hull edge (Milne et al. 1996), which is a set of the farthest points a species can reach without experiencing habitat fragmentation.

We show that the hull edge has a fractal structure and that its fractal dimension $D_f = 7/4$ depends on neither the gradient nor the step length of the species. The fractal dimension is, furthermore, the same in the GRM and the GCP and is thus insensitive to correlations introduced by a limited colonization distance. Because of this robust fractal property, we propose that the hull edge is a good can-

didate for locating and monitoring vegetation boundaries and comparing them across years, geographic regions, or biomes.

Percolation through a Landscape with an Environmental Gradient

A frequently used method for studying the connectivity structure of a landscape is percolation modeling. The main focus of percolation theory is spatial spreading in a heterogeneous medium consisting of occupied and vacant sites (Stauffer and Aharony 1994). In a typical ecological setting, an occupied site is one containing a particular habitat type (i.e., suitable for the particular organism). The significance of percolation theory for ecology was recognized in the late 1980s (Gardner et al. 1987). Since then, a number of papers have investigated habitat maps with simulations and field data (Gustafson and Parker 1992; Milne 1992; Plotnick and Gardner 1993; Loehle et al. 1996; With 1997; Li 2002; He and Hubbell 2003; Solé et al. 2005). Effects of percolation on population dynamics have also been investigated (Andrén 1994; With and Crist 1995; Bascompte and Solé 1996; Oborny et al. 2007).

A commonly used neutral model in ecology relevant to percolation is the so-called random map. In a random map, the lattice sites are occupied or vacant independently of each other. Conventionally, the map is uniform, in the sense that every site has the same probability p of being occupied (i.e., no gradient is assumed). After the set of occupied sites is determined, it is partitioned into patches, depending on the maximum step length s. All the sites belonging to the same patch can be connected by a walk that moves from one occupied site to another, taking steps no longer than s. For sites in distinct patches, no such path exists. In this article, we study patches generated for s equal to 1, 2, and 4 lattice spacings (fig. 1*A*).

Although the construction of uniform random maps (URMs) is simple, they have several intriguing properties. When the occupancy probability p is changed continuously from 0 to 1, the landscape suddenly changes from a fragmented to a connected state, that is, there is a critical value p_c at which the random map undergoes a phase transition. As p increases and approaches p_c, the average patch size S of a randomly chosen occupied site increases very rapidly. In an infinite lattice near p_c, S follows the scaling law $S \propto |p_c - p|^{-\gamma}$, with $\gamma = 43/18$ and hence diverges at p_c. Increasing p further, the probability P that a randomly chosen occupied site belongs to an infinitely large connected patch becomes larger than 0. The value of P follows a scaling law $P \propto (p - p_c)^{\beta}$, with $\beta = 5/36$. With the connected patch excluded, the average size of the fragmented patches above p_c decreases following the same scaling law as that below p_c, $S \propto |p_c - p|^{-\gamma}$.

While the existence of a sharp transition from fragmented to connected landscapes is already remarkable, it is even more surprising that the critical exponents β and γ are universal; that is, they are independent of the geometry of the lattice and the step length s. A square lattice has the same critical exponents as triangular, hexagonal, or even more complex lattices. We can even work in continuous space without referring to any underlying lattice (Meester and Roy 1996). The only factor determining the values of these exponents is the dimension of the system (Stauffer and Aharony 1994), which in landscape ecology is typically $D = 2$. Therefore, random maps possess some robust features that are insensitive to the local details of the model. (For ecological implications, see Oborny et al. 2007.)

The gradient random map (GRM) is a straightforward generalization of the URM for modeling spatial distributions along environmental gradients. We assume that the occupancy probability $p(x)$ changes with the spatial position x along a gradient. The simplest assumption is a linear function,

$$p(x) = p_0 + g_p x, \tag{1}$$

where g_p is a constant gradient (fig. 2*A*). The GRM was first introduced in statistical physics to model the diffusion of particles in a solid (Sapoval et al. 1985). In ecology, Milne et al. (1996) applied the GRM for studying the ecotone between grassland and piñon-juniper woodlands in New Mexico. They interpreted the change from fragmented to connected woodland cover as the percolating phase transition of the GRM.

To determine the precise position where the connected-to-fragmented transition occurs, it is necessary to identify the boundary, or hull edge, of the connected patch. The hull edge in the simplest case, $s = 1$, is defined as the set of all sites in the connected patch that are adjacent to exterior vacant sites (fig. 1*B*). These are vacant sites connected via nearest or next-nearest neighbors to the largest contiguous vacant area around the connected patch. Metaphorically, the hull edge is the "coastline" where the connected patch is in contact with the surrounding "ocean" of vacant sites. Interior vacant "lakes" are disregarded. The hull edge can be delineated by a left-turning biased walk along the coastline (see "Determination of the Hull Edge by a Biased Walk"). This method can also be generalized to define the hull edge for step lengths $s > 1$ (fig. 1*C*).

A common feature between our work and the study by Milne et al. (1996) is the use of various step lengths ($s = 1$ and $\sqrt{2}$ in Milne et al.; $s = 1$, 2, and 4 in our study). The results of Milne et al. clearly show a transition from a connected to a fragmented state with the decrease of woodland cover p. We develop this approach further

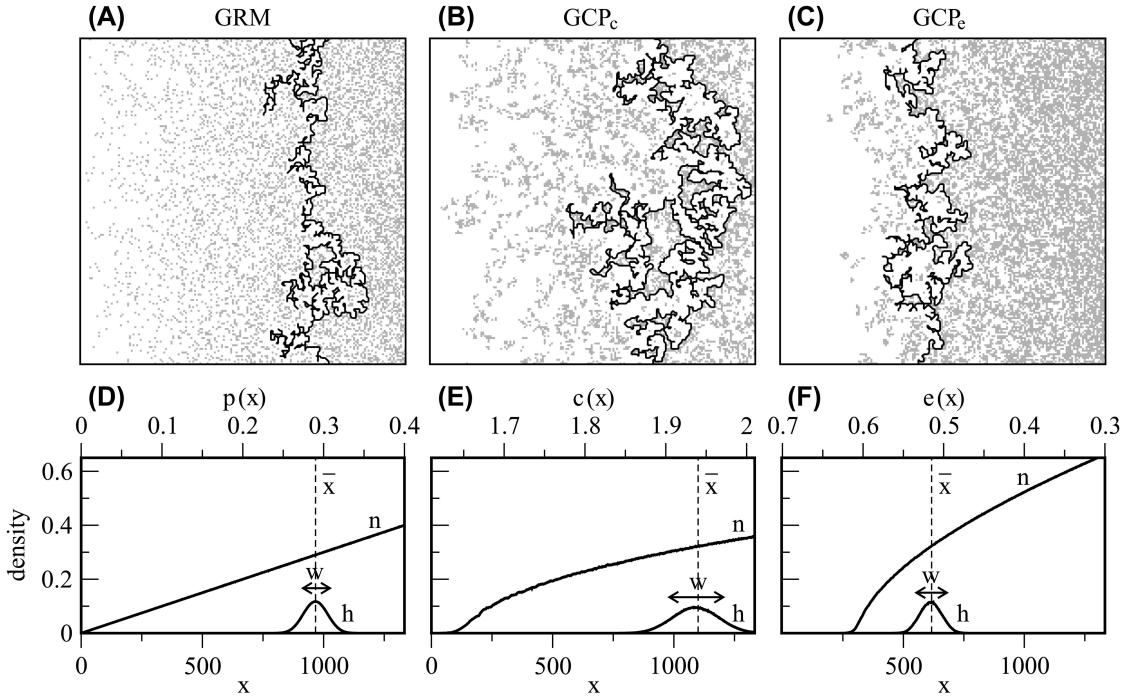

Figure 2: Comparison of the three gradient models investigated in this article. *A*, Gradient random map (GRM). *B*, Gradient contact process with linear change in the colonization rate (GCP_c). *C*, Gradient contact process with linear change in the extinction rate (GCP_e). The highlighted curves in *A–C* are the hull edges for step length $s = 2$. Occupied sites (*gray*) are less aggregated on the random map *A* than in the contact processes *B* and *C*. *D–F*, Overall population density *n* and hull density *h*, averaged over 1,000 independent realizations, for the GRM (*D*), the GCP_c (*E*), and the GCP_e (*F*). Upper horizontal axis: local values of *p*, *c*, or *e*. Lower horizontal axis: spatial position *x*.

by investigating the geometry of the hull edge for the GRM as well as other landscape models.

A Dynamic Model of Occupancy: The Contact Process

The occupation by a particular type of vegetation of a real landscape is autocorrelated, at least on some spatial scales, unlike vegetation on a random map. Several studies develop a null model by introducing a scale-free, fractal structure (e.g., Palmer 1988; Milne 1990; Plotnick et al. 1993; With et al. 1997; With and King 1999; Olff and Ritchie 2002). An alternative method is to aggregate sites on one or more spatial scales (see a review in Keitt 2000). Most approaches are static, in the sense that the generated pattern does not change over time, but some dynamic methods have also been proposed. The simplest dynamic process that creates aggregation by repeated colonization and extinction events is the so-called contact process.

Originally introduced to model contagion in epidemics (Harris 1974), the contact process has found applications in many other fields as a simple model of spatial spreading. In the context of ecology, the contact process is the simplest spatially explicit implementation of the logistic model of population growth and also of the Levins model of metapopulation growth (Levins 1969; see Dytham 2000 for a review of spatially explicit Levins models). Accordingly, several studies have used the contact process to investigate the spreading and persistence of (meta)populations in space (Barkham and Hance 1982; Crawley and May 1987; Anderson and May 1991; Durrett and Levin 1994; Levin and Durrett 1996; Holmes 1997; Franc 2004; Solé and Bascompte 2006; see Oborny et al. 2007 for a review).

In the contact process, two states of the sites are distinguished: occupied and vacant. An occupied site can colonize vacant sites in the neighborhood. The basic contact process, as introduced by Harris (1974), operates on a square lattice. The rates of colonization *c* and extinction *e* are the same in every site. Let us call this basic model without any gradient the uniform contact process (UCP). The rules described in figure 3 generate a straightforward, spatially explicit version of a logistic, or Levins, process. Although not analytically solvable, efficient numerical simulations are possible (see "Contact Process Algorithm").

To our knowledge, we are the first to apply the contact process as a model of broad-scale vegetation dynamics on

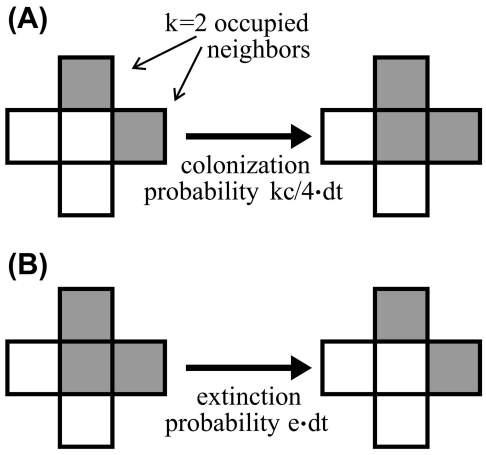

Figure 3: Updating rules in the contact process. *A*, If a site is vacant, then we count the number of occupied neighbors k in its four-site neighborhood. During a small time interval dt, the focal site becomes occupied with a probability $(kc/4) \cdot dt$. In other words, c is the rate at which one occupied site attempts to colonize any of its four neighboring sites. This neighborhood-dependent rule expresses local density dependence of the colonization process. *B*, Occupied sites become vacant (i.e., extinction occurs) with a probability $e \cdot dt$. The extinction process is assumed to be independent of the neighbors.

the landscape level. Since the contact process assumes spreading through neighborhood contacts, the only vegetation types that are suitable for this model are those in which the proximity of existing patches is important for the local community assembly, that is, in which long "jumps" are unlikely. Within this constraint, we are free to choose the spatial extent of a lattice site (i.e., the lattice constant) and the size of the neighborhood. Holland et al. (2007) have pointed out that some features of spatially explicit models can depend on the geometry of the neighborhood. However, Lennon et al. (1997) varied the neighborhood size in the uniform contact process (UCP), where c and e are the same for all sites, and concluded that several important features, such as the overall ratio of occupied to vacant sites, are rather insensitive to the neighborhood definition. Therefore, the arbitrary choice of a four-site neighborhood should not make the results too specific: they are likely to be valid, at least qualitatively, for a broader set of models. For the sake of simplicity, we consider only colonization from a four-site neighborhood (fig. 3; note that the organism that is assumed to move between the vegetation patches can step outside this neighborhood if $s > 1$).

Because we are interested in vegetation transition zones, we modify the UCP by introducing an environmental gradient. In a gradient contact process (GCP), the colonization rate c and/or the extinction rate e changes with the spatial position x. For example, $c(x)$ may vary linearly while $e(x)$ is constant,

$$c(x) = c_0 + g_c x, \qquad e(x) = 1 = \text{constant}, \tag{2}$$

or vice versa,

$$c(x) = 1 = \text{constant}, \qquad e(x) = e_0 + g_e x, \tag{3}$$

where g_c and g_e are constant gradients. We refer to the model of equation (2) as GCP_c and that of equation (3) as GCP_e. Examples are shown in figures 2*B* and 2*C*, respectively.

Both rules have been applied in metapopulation ecology for the study of range limits of species (Holt and Keitt 2000). Lennon et al. (1997) applied somewhat more complex rules for colonization, testing various neighborhood sizes and shapes. Both studies showed a phenomenon of fundamental importance: a sharp boundary may emerge even across a smooth environmental gradient. A small change in c or e can cause occupancy to decline sharply in the vicinity of the range limit. In spite of this sharpness, the boundary is not frozen but fluctuates over time (fig. 5 of Lennon et al. 1997). The standard deviation of occupancy peaks around the region where the mean shows rapid decline (Holt and Keitt 2000; Antonovics et al. 2006). Results from Lennon et al. (1997) suggest that the shape of the gradient is relatively unimportant. Changing $e(x)$ from a linear to an exponential function in equation (3) caused quantitative but not qualitative changes in the pattern of occupancy.

Our work is closely related to these studies, but we do not focus on the position x along the gradient where the vegetation vanishes. Instead, we examine the hull edge, that is, the boundary between connected and fragmented vegetation, where occupancy is still rather high. Our goal is to show that, although different models (GRM, GCP_c, GCP_e) may differ in their dynamics, spatial autocorrelations, and visual appearance (fig. 2), they have several scaling laws in common.

Numerical Simulations

We perform numerical simulations to study the GRM, GCP_c, and GCP_e models (according to eqq. [1], [2], and [3], respectively). To construct the GRM, we randomly fill all sites with the predetermined probabilities $p(x)$. To produce the GCP patterns, we let the contact process run from an initial state until equilibration (see "Removing Transients and Finite-Size Effects in the GCP" for details). Then we identify the connected patch and delineate the hull edge for step lengths $s = 1$, 2, and 4. We now present several variables to characterize the patterns.

Overall density profile. The overall density profile $n(x)$ is the number of occupied sites in column x divided by L, the number of sites in that column. (In our simulations, we use $L = 4{,}096$.) Clearly, $n(x)$ increases monotonically from unfavorable to favorable conditions. In the GRM, this change is linear (fig. 2*D*), according to equation (1). In the GCP_c and GCP_e, the emergence of the density profile is more complex. It results from dynamic colonization-extinction processes and shows a rather sharp increase from $n = 0$ to positive values of n (fig. 2*E*, 2*F*). The threshold where the transition from zero to positive density occurs is at $c(x) \approx 1.65$ in the GCP_c and $e(x) \approx 0.61$ in the GCP_e. Therefore, the rate of colonization must exceed the rate of extinction by ≈65% to enable survival. This is approximately the same value observed in the corresponding uniform contact process (Marro and Dickmann 1999).

Hull density profile. To locate the transition between connected and fragmented vegetation, we calculate the hull density $h(x)$, the fraction of sites in column x belonging to the hull edge. Despite different overall density profiles $n(x)$, $h(x)$ is in all three models bell shaped and symmetric about the maximum (fig. 2*D*–2*F*, similar to the GRM results of Milne et al. 1996). There are several tasks in which a well-defined place along the gradient has to be singled out as the "borderline" of the actual vegetation type. We propose to use the mean x-coordinate $\bar{x}$ for this purpose. It is located at rather high densities. For $s = 2$, for example, $n(\bar{x}) \approx 0.29$ (GRM) or $n(\bar{x}) \approx 0.32$ (GCP_c and GCP_e). The reason for the shift is the emergence of spatial autocorrelations in the GCPs. (Similar shifts have been observed in other correlated lattices by Mendelson [1997].) A shorter step size shifts the borderline toward a higher density. For example, in the GRM, $n(\bar{x})$ increases from 0.09 to 0.59 as s decreases from 4 to 1. It is notable that the same value, $n(\bar{x}) \approx 0.59$, was found by Milne and colleagues in a similar GRM at $s = 1$. The same authors confirmed this theoretical prediction, using empirical data from a piñon-juniper woodland edge in New Mexico (Milne et al. 1996).

Width and length of the hull. We define the width of the hull w as the standard deviation of the x-coordinates around the mean $\bar{x}$. The length of the hull u is defined as the number of lattice sites visited by the left-turning walk along the edge. We present the formal definitions of these variables and the detailed results in "Width and Length of the Hull" in the appendix. Here we summarize the main results. Larger gradients, that is, steeper slopes, or longer step lengths s lead to smaller w and u. We find that both variables scale as power laws, $w \propto g^{-4/7}$ and $u \propto g^{-3/7}$, where g stands for the gradient in the respective vegetation model (g_p, g_c, or g_e). Interestingly, the exponents depend on neither s nor the particular model, although occupied sites in the GCPs are aggregated, unlike in the GRM (see "Aggregation of the Occupied Sites in the GCPs"). The result suggests that the GCP's autocorrelations do not have any significant effect on these fundamental geometric features of the hull edge.

Fractal dimension. We calculate the fractal dimension D_f of the hull edge with the equipaced polygon method (Batty and Longley 1994; a detailed description of this method is given in "Fractal Dimension and the Equipaced Polygon Method"). The results (fig. 4) suggest the validity of scaling laws $\bar{d}(k) \propto k^{1/D_f}$, where $\bar{d}(k)$ is the average distance between k steps in the left-turning walk. Two different scaling regimes can be distinguished. For small k, the value of D_f fits 1.73 ± 0.03 (least squares fit for $16 \leq k \leq 512$); at larger values, there is a crossover to $D_f = 1$. This indicates that the hull edge is a fractal at small length scales and becomes similar to a simple straight line when viewed in coarser resolution. It is remarkable that the fractal dimension is approximately $D_f = 7/4$, and this is the same at every value of step length s and in every model (GRM, GCP_c, and GCP_e). The value $D_f = 7/4$ has been conjectured in earlier theoretical studies for the particular case of $s = 1$ and GRM (Sapoval et al. 1985). Recent mathematical work supports this conjecture (Smirnov and Werner 2001). Our results lead to the surprising conclusion that this value is not specific to the GRM or $s = 1$, and we may expect universal scaling behavior at the hull edge, independent of the exact interactions between occupied and vacant sites.

Application to Empirical Data

As an example of the hull edge of an empirical vegetation transition, we investigate the boundary of a piñon-juniper woodland on a slope of the Sandia Mountains in central New Mexico (following Milne et al. [1996], who had described the hull edge of the same vegetation type in this region). We used a high-resolution Google Earth image (fig. 5*A*) to obtain a binary matrix (748 × 1,106; fig. 5*B*), in which woody and nonwoody vegetation are distinguished. The largest (connected) woodland patch was identified, and its hull edge was outlined and analyzed by the method described for the simulated data. (See "Background Information about Figure 5*A*, 5*B*" for a detailed description of the site and of the image analysis.)

The results show remarkable similarities to the simulations. The overall density profile is half-bell shaped and suggests a rather steep slope, where n increases from low ($n \approx 0.25$) to high densities ($n \approx 0.7$) over less than 200 m (fig. 5*C*). The density of occupancy at the borderline, $n(\bar{x})$, is approximately 0.48 at $s = 2$ and 0.60 at $s = 1$. The latter is in agreement with the result of Milne et al. (1996) and with the theoretical value of the percolation

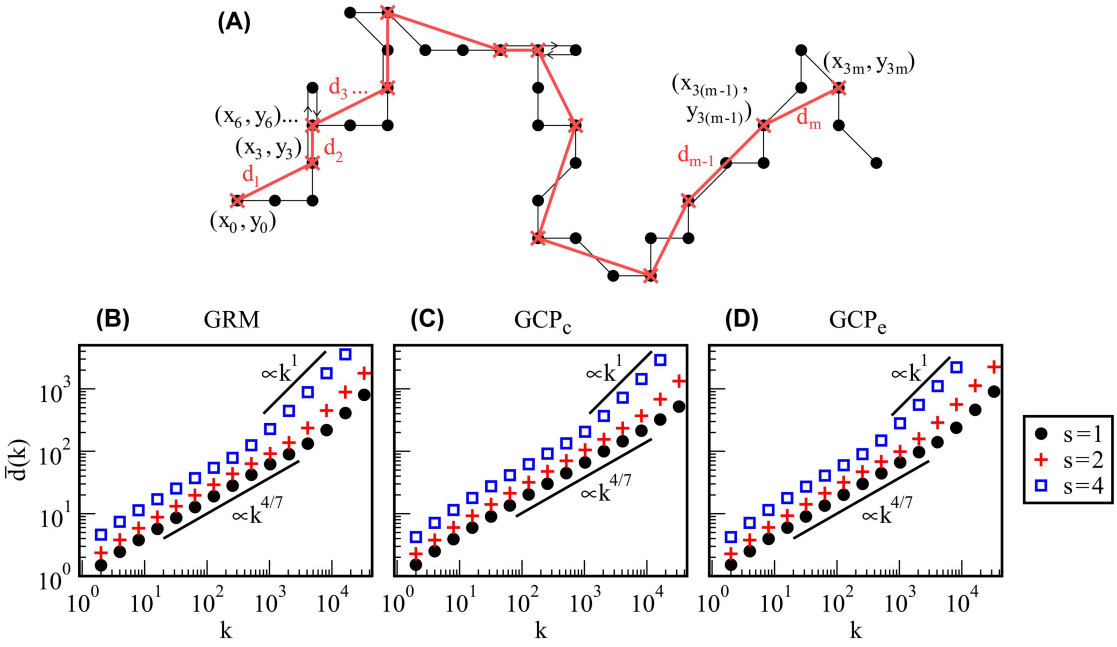

Figure 4: Fractal dimension of the hull edge. *A*, To determine the fractal dimension, we calculate the average of $(d_1, d_2, \ldots, d_m)$, the distances between k steps in the left-turning walk for a fixed number k. In *A*, $k = 3$. *B–D*, The average distance $\bar{d}(k)$ versus k on double-logarithmic axes. For small k, $\bar{d}(k)$ scales as the four-sevenths power of k, indicating a fractal dimension $D_f = 7/4$. For large k, there is a crossover to $D_f = 1$. The gradients used for the figure are $g_p = g_c = -g_e = 3 \cdot 10^{-4}$. The specific choice of the gradients influences the crossover positions between the two different scaling regimes, but the exponents remain the same for other gradients. (Each data point is the average over 10 realizations. The error bars are smaller than the symbols.)

threshold in uniform random maps at $s = 1$ (0.592746; Stauffer and Aharony 1994).

The fractal geometry of the hull in the Sandia Mountains example also shows similarities to our models. Over more than one order of magnitude, one can plausibly fit a power law, $\bar{d}(k) \propto k^{4/7}$ (fig. 5*D*). Thus, at length scales of around 10–100 m, we confirm the fractal dimension $D_f = 7/4$ that we found in our simulations. There is also a clear indication of the predicted crossover to linear scaling at large step lengths.

Discussion

Abrupt Changes along a Smooth Environmental Gradient

The delineation of vegetation zones across gradients of altitude, latitude, moisture, and so forth, is the most common way to express that discrete units of vegetation may be identified, in spite of continuous changes in the environmental background. Several studies have suggested interpreting these changes as critical phase transitions (Loehle et al. 1996; Milne et al. 1996; Wilson et al. 1996; Milne 1998; Li 2002). Our study promotes this approach: we interpret the transition from connected to fragmented vegetation as a percolation transition of a gradient contact process. We identify scaling laws for the width, length, and fractal dimension of the hull edge that characterize this transition.

The emergence of a sharp boundary is usually explained by positive feedback caused by a cooperative interaction between members of the community (Loehle et al. 1996; Milne et al. 1996; Wilson et al. 1996; Keitt et al. 2001; Li 2002; Zeng and Malanson 2006; Solé 2007). It is reasonable to assume that positive feedback would sharpen the boundary. Nevertheless, other models demonstrate that this is not a prerequisite for a sudden transition; relatively sharp borderlines can emerge even in the absence of any positive feedback. Lennon et al. (1997) and Holt and Keitt (2000) analyzed several gradient lattice models; those with linear changes in colonization or extinction rates are directly comparable with our GCPs. All these models agree that the density of occupied sites declines rapidly toward the extinction edge, yielding a half-bell-shaped curve (fig. 2*E*, 2*F*). This rapid decline is caused by a failure in the density regulation that occurs where c approaches e (Oborny et al. 2005). One of the practically important consequences is that a sharp drop in the density does not necessarily indicate that there is a similarly sharp change

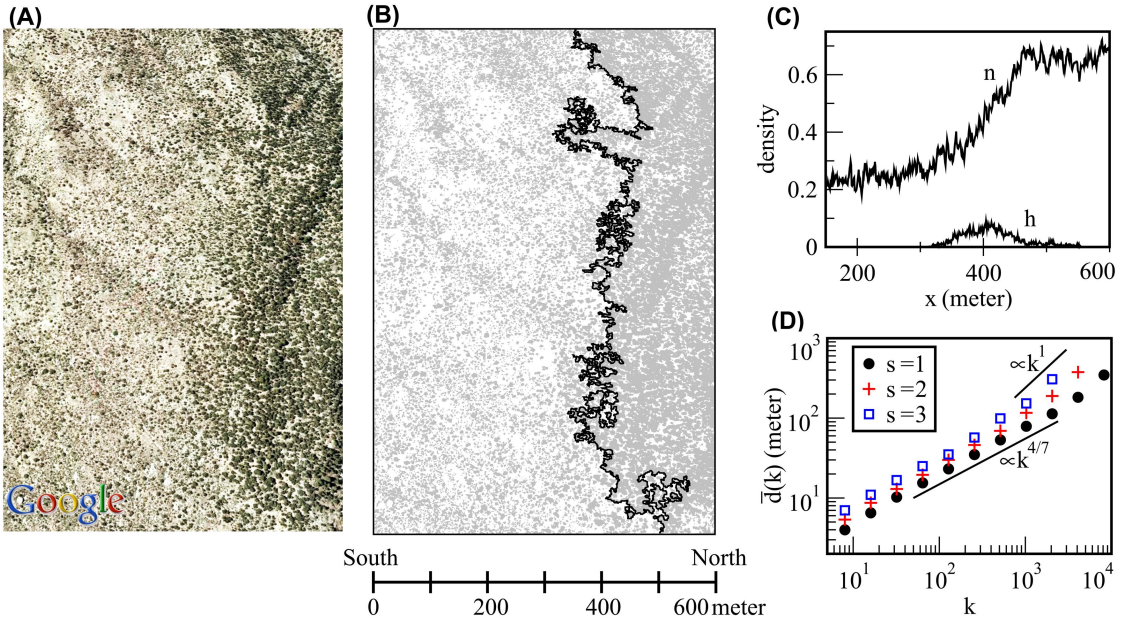

Figure 5: Edge of a piñon-juniper woodland along a slope in the Sandia Mountains (Cibola National Forest, New Mexico). *A*, Satellite image. *B*, Processed binary image. One pixel is around 80 cm × 80 cm. The hull edge for $s = 2$ is marked in black. *C*, Overall density n and hull density h as functions of position in the north-south direction. *D*, Estimation of the fractal dimension with step lengths $s = 1$, 2, or 3. The notation is the same as in figure 4.

in the environmental conditions (see also Czárán 1989; Wilson et al. 1996; Lennon et al. 1997; Wiegand et al. 2006). The tendency toward spontaneous "sharpening" suggests that vegetation boundaries can, indeed, be suitable candidates for monitoring climate change (as suggested, e.g., by Kimball and Weihrauch [2000]).

Position of the Edge

Locating the edge of a vegetation type or a species is a prerequisite for investigating several ecological problems. The working definition of the edge should be robust against microscopic (local) differences in these systems and should pinpoint some macroscopic properties of ecological importance. One obvious candidate solution is to determine the dividing line between sites of zero and nonzero occupation probability. However, this idea turns out to be impractical. A large number of samples are required to accurately determine the average density $n(x)$, especially where $n(x)$ is very small. Consider the example of a UCP on an infinite lattice. There, fluctuations are known to increase strongly at the threshold value of c/e where the vegetation vanishes, that is, where $n(x)$ becomes 0. Therefore, the size of the sample area that could statistically represent the system increases disproportionately, and so does the required observation time (see Oborny et al. 2007 for details). A gradient system cannot have infinitely large fluctuations, but the problem of increasing fluctuations toward the edge is clearly detectable (see fig. 5 in Lennon et al. 1997; Antonovics et al. 2006). Alternatively, one could consider the boundary to be the region of the steepest gradient in $n(x)$ (Timoney et al. 1993). Unfortunately, for this definition we would have to estimate the derivative of $n(x)$, which is even noisier than an estimate of n itself.

We suggest delineating the borderline between the connected and the fragmented portions of the distribution. More specifically, the borderline in our definition is the mean position $\bar{x}$ of the hull edge. Among the rich variety of methods for edge detection (see a review in Fortin et al. 2005), this method has some advantages in comparing edges across time, space, or species. First, the edge defined in this way possesses several scaling laws (width, length, and fractal dimension) that are robust, that is, insensitive to the microscopic details of the system. Second, it is relatively easy to estimate even from snapshot data. Third, statistical fluctuations are smaller near the hull edge than in the extinction zone. Fourth, edge effects, including any interference with a neighboring vegetation type, are less significant in the more internal, higher-density zone.

Several papers have emphasized the importance of a dynamic approach to range edges, in particular for investigating the causal link between local population processes

and broader-scale distribution patterns (e.g., Wilson et al. 1996; Lennon et al. 1997; Davis et al. 1998; Holt and Keitt 2000; Keymer et al. 2000; Maurer and Taper 2002; He and Hubbell 2003; Fortin et al. 2005; Guo et al. 2005; Holt et al. 2005; Parmesan et al. 2005; Travis et al. 2005; Antonovics et al. 2006; Bahn et al. 2006). In vegetation science, this connection has always been an important issue, especially in the study of patch dynamics (Pickett and White 1985; Gosz 1993). In this article, we argue that in spite of the large variety in processes and patterns, the scaling laws valid for the static GRM are also applicable to dynamic models like the GCP.

Fragmentation at the Edge: Ecotone Geometry

A decline in the occupation density necessarily brings about changes in the geometry. Studies in uniform (i.e., nongradient) systems have shown that the size distribution, isolation, perimeter/area ratio, and other geometric features of patches can significantly change with overall density (see Fahrig 2003 for a review). The same applies along a gradient, with the interesting addition that the densely occupied region can affect the sparsely occupied one. Figures 2 and 5*B* illustrate that in the transition region, "peninsulas" stretch out of the connected patch and penetrate rather deep into the fragmented region. Consequently, isolation of the fragments is less severe in gradient environments than in uniform environments with respective values of n. An additional factor that decreases isolation is fluctuation of the edge. Waves of occupancy can spread out occasionally even into a rather sparsely populated region (Lennon et al. 1997; Antonovics et al. 2006). UCP simulations (Oborny et al. 2007) and numerical experiments with the GCP (Holt and Keitt 2000) suggest that fluctuations peak around the extinction edge; therefore, this effect can be strong. It is likely that the connected patch dominates over a broad region, at least in the long run (i.e., in a dynamic view, considering decades or hundreds of years).

In "An Outlook to the Significance of Fragmentation at the Edge," we show some examples of an organism-centered view of habitat fragmentation and consider the potential consequences of the change from connected to fragmented habitat structure toward a range edge.

Robust Scaling Laws at the Edge

Many properties of a boundary are not robust against changes in the parameter values or local details of rules in the model. For example, the position, width, and length of the hull edge sensitively depend on the step length s. For a species with longer s, the hull edge shifts to lower habitat densities and becomes narrower and shorter. The gradient g also influences the hull edge: the steeper the gradient, the narrower and shorter the edge. Furthermore, the GCP produces much larger patches than the GRM (see "Aggregation of the Occupied Sites in the GCPs"). But there are three scaling laws that prove to be intriguingly robust. The width w and length u of the hull edge satisfy $w \propto g^{4/7}$ and $u \propto g^{3/7}$. Most importantly, the hull edge is a fractal with dimension $D_f = 7/4$. The values of these exponents depend on neither s nor g and are not changed by varying the local details of pattern generation. We found identical values for the GRM, the GCP_c, and the GCP_e.

Sapoval et al. (1985) proposed that the fractal dimension of the GRM is related to the critical exponents β and γ that characterize the size of the connected patch and the fragment size in the uniform process (see "Percolation through a Landscape with an Environmental Gradient") through the equation $D_f = 1 + 2/(2\beta + \gamma)$. For the known values $\beta = 5/36$ and $\gamma = 43/18$, this equation indeed yields $D_f = 7/4$. The scaling exponents for w and u can also be related to the fundamental exponents β and γ; see "Width and Length of the Hull." Since β and γ are universal (i.e., independent of the lattice), the same is true for the scaling laws for w, u, and D_f. In particular, they are also expected to be valid in correlated lattices as long as the correlations between the states of the sites (occupied or vacant) decay over short distances. This condition is met in the GCP because the hull edge is some distance away from the extinction edge, where correlations are strongest. We hypothesize that many other dynamic models would satisfy this rather weak condition, short correlation length; therefore, the same scaling laws presumably hold for a wide range of vegetation maps.

Fractal geometries generated by living organisms have been a fruitful subject of research for a long time (e.g., Palmer 1988; Milne 1990; Forman 1995; Loehle et al. 1996; Li 2002; see a general review of scaling laws in biology in Brown and West 2000 and recent reviews focusing on ecological implications: Solé and Bascompte 2006 and Storch et al. 2007). As far as we know, our study is the first exploratory step toward studying the fractal geometry of vegetation boundaries in a systematic way. This geometry is important from the aspect of ecotone effects (cf. Ims 1995) and ecological flows (Forman 1995; Wiens 1995). Several papers have emphasized the importance of the scale of animal movement (e.g., during migration or foraging) relative to the scale of habitat patches (e.g., Milne 1990; Ims 1995; Wiens 1995; Olff and Ritchie 2002). Our study provides an example for a component in the habitat pattern, the hull edge, that is scale free and therefore is likely to be perceived by different organisms in the same way.

Applicability of the Model and Further Questions

In order to observe an edge pattern emerging from colonization-extinction events, a sufficiently large area is needed relative to the distance of spreading. For example, if the vegetation can spread maximally 1 m per year under ideal conditions and the area over which the environment changes is 500 m, causing a decline from high to zero vegetation cover, then the available system size is 500 sites (lattice cells) in the x direction. This can be sufficiently large for our approach. In the transversal (y) direction, the lattice should be large enough for the estimation of the fractal dimension. The size and orientation of the lattice have to be chosen such that the hull edge spans from $y = 0$ to the maximum y-coordinate. As a rough guideline, the length should be at least 200 sites. We do not recommend testing the predictions on small (e.g., 100 × 100) lattices, because the geometric features of the hull are unlikely to be observable.

Our models are based on several simplifying assumptions. As we have pointed out, the values of the critical exponents in the scaling laws, including the fractal dimension, are expected to be robust against many kinds of modifications in the model. We list some potential factors that may change the values of the exponents or cause the scaling laws to break down.

Nonlinear changes in the environment. The environmental conditions were assumed to change linearly (eqq. [1]–[3]). This assumption rarely holds in reality, but if the change in the environmental conditions is smooth, a linear approximation may be applicable. Because the same scaling exponents are found for a linear density profile (GRM) and for two nonlinear density profiles (GCP_c and GCP_e), we believe that linearity in the environment or in the population's response is not mandatory.

Colonization distance. In our model, we assume that the vegetation spreads only to the nearest sites. The model can be readily extended by assuming that farther sites can be colonized as well, as long as the colonized neighborhood is finite or the probability of colonization decreases sufficiently fast with distance. This assumption is realistic because at least some component species are likely to be dispersal limited. If, however, self-assembly of the vegetation can take place at an arbitrary distance from existing vegetation patches, the GCP is not applicable. A modified GCP, where colonization at a randomly chosen site is attempted with rate q, interpolates between the GCP_e for $q \to 0$ and a GRM for $q \gg c$ and $e \gg c$.

Inhomogeneities. Another concern about the applicability of the model is the occurrence of an inhomogeneity in the environment in addition to the gradient already present. This is likely to occur in almost all natural landscapes; for example, depth and fertility of the soil may vary in space. According to investigations in the UCP, many properties of the contact process remain unchanged by background heterogeneity if the heterogeneous pattern is fine-grained in space and can fluctuate randomly over time, even if the frequency is very low (Szabó et al. 2002). But so-called quenched disorder (i.e., a static heterogeneity) influences the behavior of the system fundamentally, altering, for example, the time dependence of occupancy (Dickman and Moreira 1998; Szabó et al. 2002). We do not know of any study investigating the GCP with a heterogeneous background. From the existing studies on the UCP we hypothesize that heterogeneity in the environmental background would not influence the model's predictions unless the sizes of vegetation patches are smaller than the correlation length of the heterogeneity.

Nonlinear density dependence. In both the UCP and the GCP, the probability of colonizing a vacant site is proportional to the number of occupied sites in its neighborhood (fig. 3). This assumption appears to be realistic: the higher the cover of that vegetation type in the neighborhood, the higher, proportionally, is the probability of occupying the vacant site. Nevertheless, this assumption does not necessarily hold in all situations. Nonlinear density dependence may fundamentally change the behavior of the system, destroying the scaling relations completely or introducing new values for the exponents (see a review in Ódor 2004). This area is largely unknown, especially for gradients.

Memory effects. Feedback from the state of vegetation (empty vs. occupied) to the state of environment is another promising field of research. For example, a vacant site that has been occupied before can be better colonized because of soil formation, or autotoxicity by allelopathic compounds may increase the probability of extinction after some time of occupancy. Such memory effects may have consequences for the dynamics and the scaling laws.

Multiple vegetation types. Our model is a "single-species" approach, in the sense that only one vegetation type is considered and interactions between vegetation types are disregarded. This simplification may be judicious where the vegetation type under study meets bare ground (e.g., mud at a lakeshore) or dominates strongly over the alternative vegetation type. For example, an altitudinal or latitudinal tree line may be assumed (at least, in some situations) to spread until the living conditions are suitable for the trees. Predictive models about the distribution of forest vegetation often disregard the effect of the alternative, nonforest vegetation. In many cases, however, the formation of the edge may be better approximated by a "two-species" model: a struggle zone is formed by an interaction between two vegetation types. Since the hull edge is at rather high densities (fig. 2), it is possible that the struggle zone is farther away from the hull edge, so that

the existence of an alternative vegetation type does not influence predictions about scaling laws. But this condition must be checked in every two-species case. The end of the struggle zone (i.e., the farthest point at which the alternative vegetation type occurs) must not reach up to the hull edge; otherwise, both species have to be modeled simultaneously.

Conclusion

In summary, we describe and analyze two neutral models: a simple one with no spatial correlation (GRM) and a more complex one with spatial correlation (GCP). Both models are neutral, in the sense that either no interaction between the sites is assumed (in the GRM) or the interactions are assumed to be the most parsimonious (in the GCP). Both models predict a fractal dimension $D_f = 7/4$ for the hull edge and additional scaling laws for its length and width. In spite of the simplicity of these models, the scaling laws appear to be independent of the local details of the dynamics. The meaning of "local" depends on the characteristic length and time scales (correlation length and relaxation time). An example of a woodland edge in the Sandia Mountains, New Mexico, shows the applicability of the model to field data.

Acknowledgments

We thank Z. Botta-Dukát, G. Csányi, G. Meszéna, N. Moloney, G. Ódor, O. Peters, Z. Racz, and G. Szabó for discussions and helpful comments on earlier versions of this article. We appreciate the help by É. Fodor in processing the satellite image. We are grateful to B. de Gruyter and G. R. Holden of the U.S. Forest Service for a vegetation map and additional information about the vegetation in the Sandia Ranger District of the Cibola National Forest. Financial support from the Santa Fe Institute International Program and the Hungarian National Science Foundation (grant OTKA K61534) is gratefully acknowledged. G.P. gratefully acknowledges the support of a Research Councils UK Fellowship. B.O. is grateful for a Bolyai Fellowship from the Hungarian Academy of Sciences.

APPENDIX

Supplementary Material

Determination of the Hull Edge by a Biased Walk

Suppose we have identified the connected patch. Let us, for simplicity, consider $s = 1$ first. It would be inefficient to find the hull edge by determining, for every site in the connected patch, whether one of its neighbors is an exterior vacant site. This requires investigating even those sites that are deep inside the patch's interior. There is a faster algorithm that avoids investigating every site in the connected patch.

The hull edge can be interpreted as the leftmost path on the connected patch in figure 1*B* from the bottom to the top. Grossman and Aharony (1986) noticed that this latter point of view can be exploited by constructing the hull edge as a walk that stays as close to the left as possible. We start at the connected patch site in the row $y = 1$ with the smallest x-coordinate and label this position with a subscript 0; thus, $(x_0, y_0 = 1)$. Next, we attempt to walk to the site above, $(x_0, 2)$. If that site is occupied, we label it as our new position, (x_1, y_1). Otherwise, we move to the right, that is, to $(x_0 + 1, 1)$, which now has to be occupied, because $(x_0, 1)$ is in the connected patch.

With this initial seed, we begin a biased left-turning walk checking iteratively the four neighbors to the left, forward, right, and backward, in precisely this order. The direction is always measured with respect to the last move. The first occupied neighbor we find becomes our new position, labeled with a subindex equal to the number of steps taken so far. The walk terminates when we reach the leftmost connected patch site in the top row, $y = L$. At this point, all the hull sites have been visited at least once, and, conversely, all visited sites belong to the hull edge.

If $s > 1$, the species can step over a limited number of vacant sites, and the topology around the boundary of the connected patch becomes more complicated (fig. 1*C*). However, we can still define the hull edge. As before, we attempt to turn as far to the left as possible within the permitted s-neighborhood after every step. Visiting a site multiple times is permitted, but crossing our previous path is forbidden. A forbidden move is treated as if it did not exist. If there is more than one site in the same direction, we first attempt to walk to the site closest to our present location. This algorithm provides a simple, intuitive, and unique definition of the hull edge for arbitrary s. We illustrate this method for $s = 2$ in figure 1*C*.

Contact Process Algorithm

Strictly, the gradient contact process (GCP) is a continuous-time stochastic process: local colonization and extinction events are Poisson processes with rates $c(x)$ and $e(x)$ respectively, so that the waiting-time distribution for each such event is an exponential. In practice, we approximate the continuous-time process by the following discrete-time algorithm.

First, time is initialized as $t = 0$, and some arbitrary, nonempty initial configuration of occupied and vacant sites is generated on a square lattice with linear size L. Periodic boundary conditions are applied in the y-direction, so that $y = 1$ is adjacent to $y = L$. In each update,

we choose randomly one of the occupied sites, (x, y), with a rate proportional to $c(x) + e(x)$, the site's total rate of colonization and extinction. This can be implemented by determining the maximum rate $r_{max} = \max_x(c(x) + e(x))$ across the entire system, picking a site at random and accepting it for an update with probability $(c(x) + e(x))/r_{max}$. We then choose one of five processes: colonization in one of the four principal directions or extinction. Their probabilities are $(1/4) \cdot c/(c + e)$ for colonization in each of the four neighbors of (x, y) and $e/(c + e)$ for extinction. Time is then incremented by the inverse of the total rate with which sites are picked,

$$\Delta t = \left[\sum_{(x_i, y_i)\text{occupied}} (c(x_i, y_i) + e(x_i, y_i)) \right]^{-1}, \qquad \text{(A1)}$$

where the sum is over all sites occupied at time t. If we attempt to colonize an already occupied neighbor, the lattice remains unchanged. This procedure does not faithfully implement the Poissonian nature of the process, because the time increment is correct only on average, while its higher momenta are incorrect. The procedure, however, becomes exact in the limit of infinitely large systems. None of the results presented in this article relies on an exact implementation of time.

Removing Transients and Finite-Size Effects in the GCP

In the GCP, we monitor the overall instantaneous density $n(x, t) = \sum_y N(x, y, t)/L$ at all times t and for each column x, setting $N = 1$ if (x, y) is occupied at time t and $N = 0$ otherwise. In a typical run started from a random initial condition, the density will first undergo rapid changes and then stabilize, with only small fluctuations around an asymptotic temporal average value $\bar{n}(x)$.

Because we focus on time-averaged (i.e., stationary) quantities in this article, we must not include data taken before the system has equilibrated. To determine the duration of the transient, we run two simulations in parallel, one starting from a full lattice and another initialized with only 10% of the sites occupied. When the difference between the densities of the two systems is less than the standard deviation of the fluctuations around $\bar{n}(x)$ for all x, we assume that the stationary state has been reached. For the rates $c(x)$ and $e(x)$ used in this article, this point is typically reached for $100 \le t \le 1{,}000$.

Apart from possible distortions during the transient, another source of systematic errors can be caused by finite lattices. We reduce finite-size effects in two ways. First, we use large lattices ($L = 4{,}096$), so that only a small fraction of sites are on the edges of the lattice. Second, we choose periodic boundary conditions in the y-direction; that is, (x, L) is considered to be a neighbor of $(x, 1)$ for all x, so that even sites along the top and bottom edges can be colonized from two sites in the same column.

Width and Length of the Hull

After performing a left-turning walk to trace out the hull edge, the $j + 1$ coordinates of the j steps along the edge are $(x_0, y_0), (x_1, y_1), \ldots, (x_j, y_j)$. We define the mean x-position of the hull edge as

$$\bar{x} = \frac{1}{j+1} \sum_{i=0}^{j} x_i \qquad \text{(A2)}$$

and, correspondingly, the width of the hull edge as the standard deviation around the mean as

$$w = \sqrt{\frac{1}{j+1} \sum_{i=0}^{j} (x_i - \bar{x})^2}. \qquad \text{(A3)}$$

The total length of the hull edge is defined as the sum of the Euclidean distances between two consecutive steps on the edge,

$$u = \sum_{i=1}^{j} \sqrt{(x_i - x_{i-1})^2 + (y_i - y_{i-1})^2}. \qquad \text{(A4)}$$

We calculated the length u and width w of the hull edge for various gradients in the three models. Plotting the data on double-logarithmic axes (fig. A1) reveals that the width and length scale as power laws,

$$u \propto g^{-z_u},$$
$$w \propto g^{-z_w}, \qquad \text{(A5)}$$

where g stands for the gradient in the respective model, that is, g_p in the GRM, g_c in the GCP_c, and g_e in the GCP_e. Interestingly, the fitted lines suggest the same values for the exponents in the different models (GRM, GCP_c, and GCP_e) and for different step lengths s. The fitted exponents are between 0.426 and 0.434 for z_u and between 0.559 and 0.572 for z_w. For the GRM, Sapoval et al. (1985) argued that the exact values are $z_u = 3/7 = 0.428$ and $z_w = 4/7 = 0.572$, in agreement with our results. In terms of the critical percolation exponents β and γ introduced in "Percolation through a Landscape with an Environmental Gradient," the conjecture by Sapoval et al. can be expressed as $z_u = 2/(2\beta + \gamma + 2)$ and $z_w = (2\beta + \gamma)/(2\beta + \gamma + 2)$.

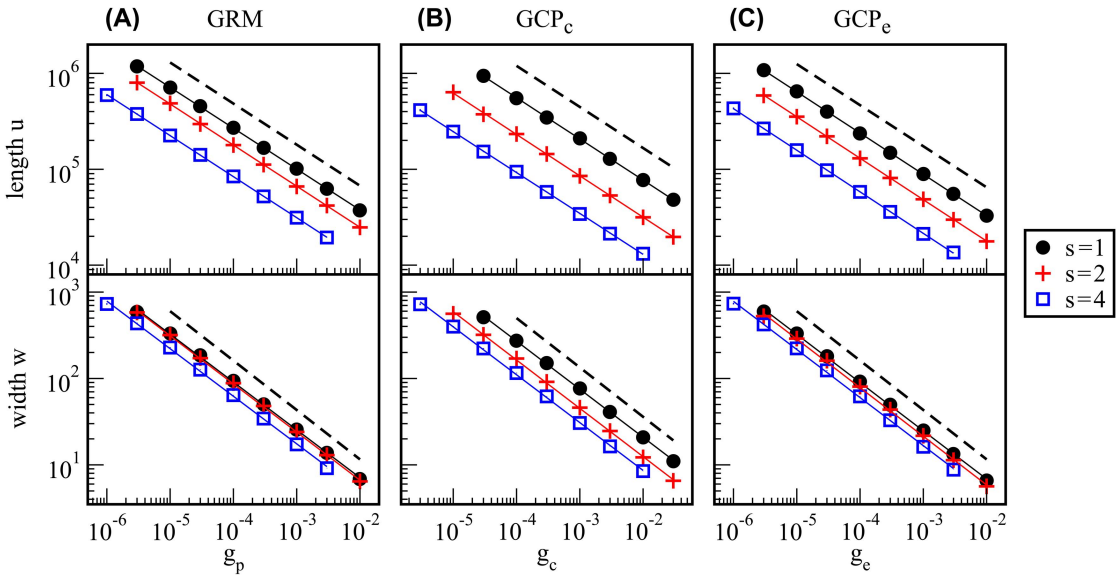

Figure A1: The length u (*top*) and width w (*bottom*) of the hull edge as a function of the gradient in the gradient random map (GRM, *A*), the gradient contact process with linear change in the colonization rate (GCP$_c$, *B*), and the gradient contact process with linear change in the extinction rate (GCP$_e$, *C*). Note that both axes are logarithmic. The dashed lines indicate the theoretical slopes −3/7 (*top*) and −4/7 (*bottom*). Each data point is an average over 200 lattices. The error bars are smaller than the symbols.

Fractal Dimension and the Equipaced Polygon Method

Since the seminal work of Mandelbrot (1982), it has become widely appreciated that many patterns in nature are best described by noninteger (i.e., fractal) dimensions. These dimensions can be determined empirically using a variety of methods, for example, by counting boxes or calculating density correlations at various length scales. In this article, we use the equipaced polygon method (Batty and Longley 1994) to determine the dimension D_f of various hull edges. This method has the advantage of being easily carried out in both computer simulations and measurements in the field.

First, we construct the hull edge as a left-turning walk, as outlined in "Determination of the Hull Edge by a Biased Walk." Let us denote the sites in the walk as $(x_0, y_0), \ldots, (x_j, y_j)$, where j is the total number of steps. Next, we repeatedly skip $k - 1$ intermediate steps and consider the distances $d_1, \ldots, d_m$ between two end points (fig. 4*A*),

$$d_1 = \sqrt{(x_k - x_0)^2 + (y_k - y_0)^2}, \ldots,$$
$$d_m = \sqrt{(x_{mk} - x_{(m-1)k})^2 + (y_{mk} - y_{(m-1)k})^2}. \quad \text{(A6)}$$

Here, m is the largest integer such that $m \le j/k$. If $mk < j$, the last few steps in the walk are ignored. We then calculate the average,

$$\bar{d}(k) = \frac{1}{m}\sum_{i=1}^{m} d_i. \quad \text{(A7)}$$

If $k = 1$, we simply have $\bar{d}(1) = u/j$, since, according to equation (A4), the distances of all j steps in the walk add up to the total length u of the hull edge. For larger k, we ignore several intermediate steps and directly connect longer distances between sites on the walk, so that $\bar{d}(k)$ increases with k. For instance, if all j steps were along a straight line, it is straightforward to show that $\bar{d}(k) \approx k\bar{d}(1)$.

The method can be generalized for geometrical objects other than straight lines. Suppose we are tracing a fractal curve with rulers of length r. Then, by definition of the fractal dimension D_f, the number of rulers N needed to get from one end of the curve to the opposite end scales as $N \propto r^{-D_f}$ (Feder 1988). If we use the step sizes in the biased walk as our rulers, we have a varying ruler length, and only on average $r = \bar{d}(k)$. The number of these rulers is $N = m$, so that $m \propto \bar{d}(k)^{-D_f}$. For a fixed number of steps j, m scales as k^{-1}, and we arrive at $\bar{d}(k) \propto k^{1/D_f}$. Thus, a double-logarithmic plot of $\bar{d}(k)$ versus k should yield a straight line, as in figure 4*B*–4*D*. The inverse of its slope is the fractal dimension D_f.

Aggregation of the Occupied Sites in the GCPs

To demonstrate that the GCP produces an aggregated distribution of occupied sites, we define two reference models, GRM_c and GRM_e, in which each column in the lattice is occupied with the same mean density $n(x)$ as in the GCP_c and GCP_e (shown in fig. 2*E*, 2*F*) but the occupied sites are randomized within each column. The GRM_c and GRM_e are thus random maps with nonlinear density profiles, in which the occupied and empty sites are uncorrelated.

As a measure of fragmentation, we calculate the average patch size of a randomly chosen occupied site with coordinate x. We exclude the sites in the connected patch because the size of this patch diverges. Formally, we define the fragment size as $S(x) = \sum_{y=1}^{L} F(x, y)/G(x)$, where $F(x, y)$ is the number of sites in the same fragment as (x, y) and $G(x)$ is the number of all sites in row x that are a part of a fragment.

A comparison between the patch sizes S in the two GCPs and the corresponding random references is shown in figure A2. The maximum of S in both the GCP_c and the GCP_e is more than twice as large as that for the corresponding random reference, indicating spatial aggregation. The aggregation is caused by dispersal limitation, that is, the constraint that only neighboring sites can be colonized. Whenever the neighborhood is finite, this phenomenon will occur.

*Background Information about Figure 5*A, *5*B

To demonstrate the application of the method on a real vegetation pattern, we searched for a region on Google Earth where a tree line is clearly visible in fine resolution and the slope is rather even (i.e., the topography does not vary too much perpendicularly to the gradient, in the y-direction). We chose a boundary of a piñon-juniper woodland in the Sandia Ranger District of Cibola National Forest (35°13′30″N latitude, 106°28′30″W longitude). The size of the area is approximately 600 m × 900 m, with forest cover increasing from south to north, that is, from downhill to uphill, according to increasing moisture. A specific advantage of the site is that Milne et al. (1996) studied the hull edge of the same vegetation type in the same district. The satellite image (fig. 5*A*) was converted from JPEG format into a binary map (woodland vs. nonwoodland; fig. 5*B*) by using Otsu's (1979) method. This procedure resulted in a 748 × 1,106 binary matrix, which was analyzed with the same methods as used for the analysis of the simulated patterns. There was only a minor difference: periodic boundary conditions were not applicable on the real-life map. We identified the largest (connected) patch, marked its hull edge at different step lengths ($s = 1$, 2, or 3), and estimated the fractal dimension in the 10–100-m range.

An Outlook to the Significance of Fragmentation at the Edge

Before deciding whether a landscape is connected or fragmented in practice, we need to have an estimate for s, the movement range of the actual species under study (cf. Forman 1995; Ims 1995; With and Crist 1995; With et al. 1997; Wiens 1997; Bunn et al. 2000; Solé and Bascompte 2006). For example, brown kiwi (*Apteryx australis*) has been observed to cross 80 m between forest patches readily, but greater distances significantly decreased the chance of colonization; a 500-m distance proved to be impassable (Potter 1990). A flying bird species, the Mexican spotted owl (*Strix occidentalis lucida*), was estimated to disperse over >45 km, and it was found that, at least in some parts of the range, juveniles can establish new territories 10–20 km away from their natal territory. Keitt et al. (1997) analyzed percolation properties of the bird's nesting hab-

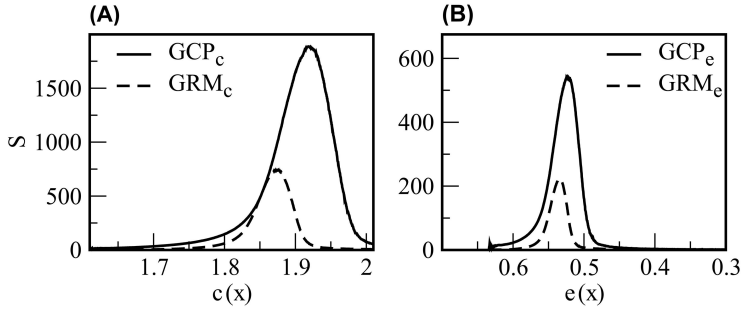

Figure A2: Fragment sizes S for the gradient contact process and gradient random map with linear change in the colonization rate (GCP_c and GRM_c, respectively; *A*) and the gradient contact process and gradient random map with linear change in the extinction rate (GCP_e and GRM_e, respectively; *B*). The parameters are the same as in figure 2*E*, 2*F*.

itat, mixed conifer forests and ponderosa pine forests in the southwestern United States, and concluded that the actual landscape went from a fragmented to a connected phase as the dispersal distance exceeded 45 km. It is interesting to link these results with our dynamic model, the GCP, where the connected and fragmented phase occur on the same map. The hull edge represents the margin of the forest types required by the species.

The chance to spread from the mainland to habitat islands and back may have serious consequences for the occurrence of genetic drift in the islands (Vucetich and Waite 2003) and for local adaptation (Bahn et al. 2006; for a review, see Goldberg and Lande 2007). Increasing habitat fragmentation at the range margin was observed, for example, in three amphibian species (spotted salamander, wood frog, and red-spotted newt) in Connecticut (Gibbs 1998). Our study underlines that a "snapshot"-type study of isolation may be insufficient whenever splitting and merging between islands and mainland can occur, typically in a dynamic habitat. While the hull edge can be delineated from snapshot data, the degree of isolation of individual sites can be assessed only from repeated samplings over time.

Another important consequence of habitat fragmentation at the edge is a transition from traditional population dynamics to metapopulation dynamics. Figure 1*B*, 1*C* illustrate that the same place along gradient x can provide connected habitat for one species but fragmented habitat for another with a smaller step length. A difference in habitat connectivity may affect competitive hierarchy. For example, Brown (1971) found that tree density was a key factor in determining the result of competition between two chipmunk species. *Eutamias dorsalis* excluded *Eutamias umbrinus* in sparse piñon-juniper woodlands because *E. dorsalis* was better at moving across open ground and chasing away its competitor with aggressive attacks. In denser forests, however, *E. umbrinus* could move between trees to avoid attacks, and the competitive hierarchy turned: *E. umbrinus* excluded *E. dorsalis*.

Community diversity is also expected to change along the gradient (cf. Solé et al. 2004). The effect of decreasing habitat density is straightforward; the effect of a concomitant fragmentation requires more careful consideration. Fahrig (2003) unraveled these two factors and reviewed a large number of empirical studies on uniform (i.e., nongradient) landscapes. In all studies, she found that decreased density ("habitat loss") reduces biodiversity but that the effect of fragmentation is ambiguous: both increase and decrease have been observed. A traditional island biogeographic reasoning would predict species loss in smaller and more distant patches. Furthermore, many species are known to require a minimal patch size for survival. For example, the bog fritillary butterfly was estimated to require a 0.2-ha minimal patch area to establish a local population in a highly fragmented landscape in Belgium (Mennechez et al. 2003). Edge effects are twofold: some species react negatively and others positively to edges (Fahrig 2003). Partially isolated patches may provide temporary refugia for prey against predators, hosts against parasites, or subordinate species against dominant competitors, stabilizing their coexistence (see Durrett and Levin 1994; Czárán 1997; Nee et al. 1997; Fahrig 2003; Solé and Bascompte 2006 and references therein). The uncertainty about whether fragmentation has a net positive or negative effect is expressed in the "single large or several small" debate in conservation biology (Primack 1998). We do not suggest any general solution but merely point out that the transition from high to low connectivity is abrupt in a gradient situation. The sizes and shapes of individual patches and their degrees of isolation change dynamically.

Naturally, not only the occupied area but also the vacant area can be viewed as a habitat. Gap structure was studied with a uniform percolation model in a rainforest in Panama (Solé et al. 2005). Complementary information (about gap structure and patch structure) would be important in a variety of landscapes, because in an autocorrelated case (e.g., in a UCP or a GCP), the statistics of occupied patches cannot be expected to be the same as the statistics of the vacant patches (unlike those in a URM or a GRM).

Literature Cited

Allen, C. D., and D. D. Breshears. 1998. Drought-induced shift of a forest-woodland ecotone: rapid landscape response to climate variation. Proceedings of the National Academy of Sciences of the USA 95:14839–14842.

Anderson, R. M., and R. M. May. 1991. Infectious diseases and control. Oxford University Press, Oxford.

Andrén, H. 1994. Effects of habitat fragmentation on birds and mammals in landscapes with different proportions of suitable habitat: a review. Oikos 71:355–366.

Antonovics, J., A. J. McKane, and T. J. Newman. 2006. Spatiotemporal dynamics in marginal populations. American Naturalist 167: 16–27.

Bahn, V., J. O'Connor, and W. B. Krohn. 2006. Effect of dispersal at range edges on the structure of species ranges. Oikos 115:89–96.

Barkham, J. P., and C. E. Hance. 1982. Population dynamics of the wild daffodil (*Narcissus pseudonarcissus*). III. Implications of a computer model of 1000 years of population change. Journal of Ecology 70:323–344.

Bascompte, J., and R. V. Solé. 1996. Habitat fragmentation and extinction thresholds in spatially explicit models. Journal of Animal Ecology 65:465–473.

Batty, M., and P. Longley. 1994. Fractal cities. Academic Press, London.

Brown, J. H. 1971. Mechanisms of competitive exclusion between two species of chipmunks. Ecology 52:305–311.

Brown, J. H., and G. B. West, eds. 2000. Scaling in biology. Oxford University Press, Oxford.

Bunn, A. G., D. L. Urban, and T. H. Keitt. 2000. Landscape con-

nectivity: a conservation application of graph theory. Journal of Environmental Management 59:265–278.

Crawley, M. J., and R. M. May. 1987. Population dynamics and plant community structure: competition between annuals and perennials. Journal of Theoretical Biology 125:475–489.

Czárán, T. 1989. Coexistence of competing populations along environmental gradients: a simulation study. Coenoses 4:113–120.

———. 1997. Spatiotemporal models of population and community dynamics. Chapman & Hall, New York.

Danby, R. K., and D. S. Hik. 2007. Variability, contingency and rapid change in recent subarctic alpine tree line dynamics. Journal of Ecology 95:352–363.

Davis, A. J., L. S. Jenkinson, J. H. Lawton, B. Shorrocks, and S. Wood. 1998. Making mistakes when predicting shifts in species range in response to global warming. Nature 391:783–786.

Dickman, R., and A. G. Moreira. 1998. Violation of scaling in the contact process with quenched disorder. Physical Review E 57: 1263–1268.

Durrett, R., and S. A. Levin. 1994. Stochastic spatial models: a user's guide to ecological applications. Philosophical Transactions of the Royal Society B: Biological Sciences 343:329–350.

Dytham, C. 2000. Habitat destruction and extinctions: predictions from metapopulation models. Pages 315–331 *in* M. J. Hutchings, E. A. John, and A. J. A. Stewart, eds. The ecological consequences of environmental heterogeneity. Cambridge University Press, Cambridge.

Fahrig, L. 2003. Effects of habitat fragmentation on biodiversity. Annual Review of Ecology, Evolution, and Systematics 34:487–515.

Feder, J. 1988. Fractals. Plenum, New York.

Forman, R. T. T. 1995. Land mosaics: the ecology of landscapes and regions. Cambridge University Press, Cambridge.

Fortin, M.-J., T. H. Keitt, B. A. Maurer, M. L. Taper, D. M. Kaufman, and T. M. Blackburn. 2005. Species' geographic ranges and distributional limits: pattern analysis and statistical issues. Oikos 108: 7–17.

Franc, A. 2004. Metapopulation dynamics as a contact process on a graph. Ecological Complexity 1:49–63.

Gardner, R. H., B. T. Milne, M. G. Turner, and R. V. O'Neill. 1987. Neutral models for the analysis of broad-scale landscape pattern. Landscape Ecology 1:19–28.

Gibbs, J. P. 1998. Distribution of woodland amphibians along a forest fragmentation gradient. Landscape Ecology 13:263–268.

Goldberg, E. E., and R. Lande. 2007. Species' borders and dispersal barriers. American Naturalist 170:297–304.

Gosz, J. R. 1993. Ecotone hierarchies. Ecological Applications 3:369–376.

Grossman, T., and A. Aharony. 1986. Structure and perimeters of percolation clusters. Journal of Physics A 19:L745–L751.

Guo, Q., M. Taper, M. Schoenberger, and J. Brandle. 2005. Spatial-temporal population dynamics across species range: from centre to margin. Oikos 108:47–57.

Gustafson, E. J., and G. R. Parker. 1992. Relationships between landcover proportion and indices of landscape spatial pattern. Landscape Ecology 7:101–110.

Harris, T. E. 1974. Contact interactions on a lattice. Annals of Probability 2:969–988.

He, F., and S. P. Hubbell. 2003. Percolation theory for the distribution and abundance of species. Physical Review Letters 91:198103.

Holland, E. P., J. N. Aegerter, C. Dytham, and G. C. Smith. 2007. Landscape as a model: the importance of geometry. PLoS Computational Biology 3:e200.

Holmes, E. 1997. Basic epidemiological concepts in a spatial context. Pages 111–136 *in* D. Tilman and P. Kareiva, eds. Spatial ecology: the role of space in population dynamics and interspecific interactions. Princeton University Press, Princeton, NJ.

Holt, R. D., and T. H. Keitt. 2000. Alternative causes for range limits: a metapopulation perspective. Ecology Letters 3:41–47.

Holt, R. D., B. A. Maurer, M. L. Taper, M. A. Lewis, and T. H. Keitt. 2005. Theoretical models of species' borders: single species approaches. Oikos 108:18–27.

Ims, R. A. 1995. Movement patterns related to spatial structures. Pages 85–109 *in* L. Hansson, L. Fahrig, and G. Merriam, eds. Mosaic landscapes and ecological processes. Chapman & Hall, London.

Keitt, T. H. 2000. Spectral representation of neutral landscapes. Landscape Ecology 15:479–493.

Keitt, T. H., D. L. Urban, and B. T. Milne. 1997. Detecting critical scales in fragmented landscapes. Conservation Ecology 1:4.

Keitt, T. H., M. A. Lewis, and R. D. Holt. 2001. Allee effects, invasion pinning, and species' borders. American Naturalist 157:203–216.

Keymer, J. E., P. A. Marquet, J. X. Velasco-Hernández, and S. A. Levin. 2000. Extinction thresholds and metapopulation persistence in dynamic landscapes. American Naturalist 156:478–494.

Kimball, K. D., and D. M. Weihrauch. 2000. Alpine vegetation communities and the alpine-treeline ecotone boundary in New England as biomonitors for climate change. Pages 93–101 *in* S. F. McCool, D. N. Cole, W. T. Borrie, and J. O'Loughlin, eds. Wilderness science in a time of change. Vol. 3. Wilderness as a place for scientific inquiry. Proceedings RMRS-P-15-VOL-3. USDA, Forest Service, Rocky Mountain Research Station, Ogden, UT.

Lennon, J. J., J. R. G. Turner, and D. Connell. 1997. A metapopulation model of species boundaries. Oikos 78:486–502.

Levin, S. A., and R. Durrett. 1996. From individuals to epidemics. Philosophical Transactions of the Royal Society B: Biological Sciences 351:1615–1621.

Levins, R. 1969. Some demographic and genetic consequences of environmental heterogeneity for biological control. Bulletin of the Entomological Society of America 15:237–240.

Li, B.-L. 2002. A theoretical framework of ecological phase transitions for characterizing tree-grassland dynamics. Acta Biotheoretica 50: 141–154.

Loehle, C., B.-L. Li, and R. C. Sundell. 1996. Forest spread and phase transitions at forest-prairie ecotones in Kansas, U.S.A. Landscape Ecology 11:225–235.

Mandelbrot, B. B. 1982. The fractal geometry of nature. W. H. Freeman, San Francisco.

Marro, J., and R. Dickmann. 1999. Nonequilibrium phase transitions in lattice models. Cambridge University Press, Cambridge.

Maurer, B. A., and M. L. Taper. 2002. Connecting geographical distributions with population processes. Ecology Letters 5:223–231.

Meester, R., and R. Roy. 1996. Continuum percolation. Cambridge University Press, Cambridge.

Mendelson, K. S. 1997. Percolation threshold of a class of correlated lattices. Physical Review E 56:6586–6588.

Mennechez, G., N. Schtickzelle, and M. Baguette. 2003. Metapopulation dynamics of the bog fritillary butterfly: comparison of demographic parameters and dispersal between a continuous and a highly fragmented landscape. Landscape Ecology 18:279–291.

Milne, B. T. 1990. Lessons from applying fractal models to landscape

patterns. Pages 199–239 *in* M. G. Turner and R. H. Gardner, eds. Quantitative methods in landscape ecology: the analysis and interpretation of landscape heterogeneity. Springer, New York.

———. 1992. Spatial aggregation and neutral models in fractal landscapes. American Naturalist 139:32–57.

———. 1998. Motivation and benefits of complex systems approaches in ecology. Ecosystems 1:449–456.

Milne, B. T., T. H. Keitt, C. A. Hatfield, J. David, and P. T. Hraber. 1996. Detection of critical densities associated with piñon-juniper woodland ecotones. Ecology 77:805–821.

Nee, S., R. M. May, and M. P. Hassell. 1997. Two-species metapopulation models. Pages 123–147 *in* I. Hanski and M. Gilpin, eds. Metapopulation biology: ecology, genetics, and evolution. Academic Press, San Diego, CA.

Oborny, B., G. Meszéna, and G. Szabó. 2005. Dynamics of populations on the verge of extinction. Oikos 109:291–296.

Oborny, B., G. Szabó, and G. Meszéna. 2007. Survival of species in patchy landscapes: percolation in space and time. Pages 409–440 *in* D. Storch, P. Marquet, and J. Brown, eds. Scaling biodiversity. Ecological Reviews. Cambridge University Press, Cambridge.

Ódor, G. 2004. Universality classes in nonequilibrium lattice systems. Reviews of Modern Physics 76:663–724.

Olff, H., and M. E. Ritchie. 2002. Fragmented nature: consequences for biodiversity. Landscape and Urban Planning 58:83–92.

Otsu, N. 1979. A threshold selection method from gray-level histograms. IEEE Transactions on Systems, Man and Cybernetics 9: 62–66.

Palmer, M. W. 1988. Fractal geometry: a tool for describing spatial patterns of plant communities. Plant Ecology 75:91–102.

Parmesan, C., S. Gaines, L. Gonzalez, D. M. Kaufman, J. Kingsolver, A. T. Peterson, and R. Sagarin. 2005. Empirical perspectives on species borders: from traditional biogeography to climate change. Oikos 108:58–75.

Pickett, S. T. A., and P. S. White, eds. 1985. The ecology of natural disturbance and patch dynamics. Academic Press, New York.

Plotnick, R. E., and R. H. Gardner. 1993. Lattices and landscapes. Lectures on Mathematics in the Life Sciences 23:129–157.

Plotnick, R. E., R. H. Gardner, and R. V. O'Neill. 1993. Lacunarity indices as measures of landscape texture. Landscape Ecology 8: 201–211.

Potter, M. A. 1990. Movement of North Island brown kiwi (*Apteryx australis mantelli*) between forest remnants. New Zealand Journal of Ecology 14:17–24.

Primack, R. B. 1998. Essentials of conservation biology. Sinauer, Sunderland, MA.

Sapoval, B., M. Rosso, and J. F. Gouyet. 1985. The fractal nature of a diffusion front and relation to percolation. Journal de Physique Lettres 46:149.

Smirnov, S., and W. Werner. 2001. Critical exponents for two-dimensional percolation. Mathematical Research Letters 8:729–744.

Solé, R. V. 2007. Scaling laws in the drier. Nature 449:151–153.

Solé, R. V., and J. Bascompte. 2006. Self-organization in complex ecosystems. Monographs in Population Biology 42. Princeton University Press, Princeton, NJ.

Solé, R. V., D. Alonso, and J. Salda. 2004. Habitat fragmentation and biodiversity collapse in neutral communities. Ecological Complexity 1:65–75.

Solé, R. V., F. Bartumeus, and G. P. Gamarra. 2005. Gap percolation in rainforests. Oikos 110:177–185.

Stauffer, D., and A. Aharony. 1994. Introduction to percolation theory. Taylor & Francis, London.

Storch, D., P. A. Marquet, and J. Brown, eds. 2007. Scaling biodiversity. Ecological Reviews. Cambridge University Press, Cambridge.

Szabó, G., H. Gergely, and B. Oborny. 2002. Generalized contact process on random environments. Physical Review E 65:066111.

Timoney, K. P., G. H. La Roi, and M. R. T. Dale. 1993. Subarctic forest-tundra vegetation gradients: the sigmoid wave hypothesis. Journal of Vegetation Science 4:387–394.

Travis, J. M. J., R. W. Brooker, and C. Dytham. 2005. The interplay of positive and negative species interactions across an environmental gradient: insights from an individual-based model. Biology Letters 1:5–8.

Vucetich, J. A., and T. A. Waite. 2003. Spatial patterns of demography and genetic processes across the species' range: null hypotheses for landscape conservation genetics. Conservation Genetics 4:639–645.

Whittaker, R. H. J., and W. A. Niering. 1965. Vegetation of the Santa Catalina Mountains, Arizona: a gradient analysis of the south slope. Ecology 46:429–452.

Wiegand, T., J. J. Camarero, N. Rüger, and E. Gutiérrez. 2006. Abrupt population changes in treeline ecotones along smooth gradients. Journal of Ecology 94:880–892.

Wiens, J. A. 1995. Landscape mosaics and ecological theory. Pages 1–27 *in* L. Hansson, L. Fahrig, and G. Merriam, eds. Mosaic landscapes and ecological processes. Chapman & Hall, London.

———. 1997. Metapopulation dynamics and landscape ecology, Pages 43–68 *in* I. Hanski and M. E. Gilpin, eds. Metapopulation biology: ecology, genetics, and evolution. Academic Press, San Diego, CA.

Wilson, W. G., R. M. Nisbet, A. H. Ross, C. Robles, and R. A. Desharnais. 1996. Abrupt population changes along smooth environmental gradients. Bulletin of Mathematical Biology 58:907–922.

With, K. A. 1997. The application of neutral landscape models in conservation biology. Conservation Biology 11:1069–1080.

With, K. A., and T. O. Crist. 1995. Critical thresholds in species' responses to landscape structure. Ecology 76:2446–2459.

With, K. A., and A. W. King. 1999. Extinction thresholds for species in fractal landscapes. Conservation Biology 13:314–326.

With, K. A., R. H. Gardner, and M. G. Turner. 1997. Landscape connectivity and population distributions in heterogeneous environments. Oikos 78:151–169.

Zeng, Y., and G. P. Malanson. 2006. Endogenous fractal dynamics at alpine treeline ecotones. Geographical Analysis 38:271–287.

Associate Editor: Uta Berger
Editor: Donald L. DeAngelis